STRUCTURAL DEFORMATION ANALYSIS ON MORPHING MAV WING

Noor Iswadi Ismail, M. Hisyam Basri*, Mahadzir M.M, Hazim Sharudin, Sharzali Che Mat, Muhammad Arif Ab Hamid Pahmi, Azmi Husin and Rozaini Othman

Mechanical Engineering Studies, College of Engineering, Universiti Teknologi MARA, Cawangan Pulau Pinang, Kampus Permatang Pauh, Penang, Malaysia.

*Corresponding email: mhisyam.mbasri@uitm.edu.my

Article history
Received
3rd February 2023
Revised
18th October 2023
Accepted
6th November 2023
Published
1st December 2023

ABSTRACT

Micro air vehicles (MAV) and the notion of morphing are always changing to suit their mission characteristics. To achieve twist morphing, however, the process underlying the application of the morphing force and its related aerodynamic load is not well understood. In this study, the structural deformation of the washout twist morphing wing MAV was investigated, and the association between wing deformation, morphing force, and membrane inflation owing to aerodynamic force was clarified. Several numerical simulations of washout TM wings were undertaken and compared to those of rigid and membrane wings. The results demonstrated that twist morphing is associated with considerable wing deformation. In comparison to the TM 3N, TM 1N, and baseline wing, the TM 5N wing was the most distorted. The deformation of the wing structure was substantially influenced by the morphing force applied to the wing. Larger morphing power led to a greater degree of wing distortion.

Keywords: *Micro air vehicle, Twist morphing wing*

1.0 INTRODUCTION

Innovation knows no bounds in the aviation industry. The rise of Micro Air Vehicles (MAVs) demonstrates the relentless pursuit of smaller, more agile aircraft. MAVs, which are derived from the rapid development of Unmanned Aerial Vehicles (UAVs), are revolutionizing aerial missions due to their small size and enhanced agility.

A Micro Air Vehicle, also known as an smaller version of UAV[1], is the most recent generation of aircraft. It is a direct result of the growing demand for smaller, more agile platforms in the realm of UAVs. Its compact size and unparalleled agility set it apart, making it an ideal choice for a variety of missions. To provide context, an MAV typically has a wingspan of 6 inches[2] (approximately 15 cm), a maximum velocity of less than 15 m/s[3], and an overall weight of less than 1 kg[4]. To truly understand the significance of MAVs, it is necessary to first understand their origins in the evolution of UAVs. UAVs have rapidly altered the aviation landscape. These pilotless aircraft have proven to be extremely useful in a variety of applications ranging from military reconnaissance[5] to disaster relief. The demand for smaller, more maneuverable UAVs, on the other hand, drove the development of MAVs[6].

One of the distinguishing features of MAVs is their increased agility. Their small size and lightweight[7] construction allow them to perform intricate maneuvers[8] with remarkable precision. This agility is especially useful in environments where larger UAVs would struggle to navigate[9]. As a result, MAVs are increasingly being used in situations that require quick and precise[10] actions. Another notable feature of MAVs is their versatility[11]. Their small stature

 DOI: https://doi.org/10.11113/jm.v46.488

and agility open up a world of possibilities in a variety of domains. MAVs are used for reconnaissance, surveillance, and even as decoy drones in military operations. Their ability to enter confined spaces and gather real-time intelligence makes them invaluable assets on the battlefield. MAVs are used in search and rescue missions outside of the military. Their small size allows them to easily navigate through debris and collapsed structures, assisting in the search for survivors and assessing disaster-stricken areas. MAVs also play a role in environmental monitoring, assisting scientists in gathering data from remote or inaccessible locations.

MAVs are not without challenges, despite their impressive capabilities. These miniature aircraft's limited payload capacity limits their endurance and range. Furthermore, their small size makes incorporating advanced sensors and communication systems difficult. Researchers and engineers are working hard to overcome these limitations so that MAVs can reach their full potential. Several of MAV designed, built and flight tested by Torres and Mueller[12], Chen et. al [13], Phan et al.[14], and Abdulrahim[15] were successful and efficacious.

Due to their diminutive size and nimbleness, Micro Air Vehicles (MAVs) are ushering in a new age of aerial capabilities. These compact aircraft have evolved as a result of the rapid advancements in unmanned aviation technology, which have necessitated the development of innovative solutions to overcome inherent difficulties. The incorporation of morphing wing concepts, in which the wing's geometry changes during flight to address multiple critical problems, is one example of such a solution. This article explores how this cutting-edge technology can revolutionize the design of MAVs by mitigating flow separation bubbles, large wing tip vortex swirling systems, challenging flight control, and issues associated with small center of gravity (CG) locations.

Flow separation occurs when the airflow passing over an airfoil separates from its surface, resulting in a loss of lift and increased drag. Mitigating flow separation is critical for sustained performance in MAVs, which frequently operate in challenging flight conditions. MAVs can adjust their wing profiles in real time thanks to morphing wing technology, which reduces the risk of flow separation. MAVs can maintain optimal lift and minimize drag by dynamically adjusting the wing's camber and other parameters, thereby improving overall aerodynamic efficiency.

Large wing tip vortex swirling systems are a common problem in traditional fixed-wing aircraft, resulting in increased drag and decreased efficiency. Morphing wing technology provides an elegant solution in MAVs, where every ounce of energy counts. MAVs can reduce the generation and impact of wing tip vortices by changing the shape of the wingtips during flight. This improves not only aerodynamic performance but also maneuverability and the energy required for sustained flight.

Difficult flight control poses a significant challenge for MAVs, especially in adverse weather or complex mission environments. Morphing wings can alleviate this burden by actively adjusting the aerodynamic properties of the aircraft. Better balance and stability result from the ability to redistribute aerodynamic loads across the wings. As a result, MAVs with morphing wings have better flight control, even in turbulent or gusty conditions. This translates to more accurate and dependable mission execution.

MAV payload capacity is frequently limited, resulting in small center of gravity (CG) locations that can affect stability. Morphing wing technology allows for CG adjustment while in flight. MAVs can maintain stability with varying payloads or equipment by strategically shifting the CG position. This adaptability ensures that the aircraft remains responsive and balanced in the face of mission-specific requirements.

Morphing wing technology represents a paradigm shift in aviation design. Unlike traditional fixed-wing configurations, morphing wings are designed to adapt and change shape during flight, dynamically responding to varying aerodynamic conditions. When applied to MAVs, this concept provides unprecedented advantages, including the ability to compensate for some of their inherent limitations. Therefore, it is very important to introduce the morphing capability on MAV in view to further improving the flying platform.

This paper considers the introduction of washout twist morphing to a MAV's wing. The actual morphing is quite straightforward and generates from twisting the wing tips by imposing a

 DOI: https://doi.org/10.11113/jm.v46.488

certain magnitude of forces. A two-way fluid structure interaction (FSI) investigation which consists of a quasistatic aeroelastic structural analysis coupled with 3D incompressible Reynolds-averaged Navier–Stokes and shear-stress-transport (RANS–SST) solver was used in this study. It could be argued that the use of two-way coupling fluid structure interaction is unwarranted for wing structure deformation analysis but is essentially impossible to actually develop and estimate the pre-deformed MAV wing since membrane and aerodynamic force are considered in the study. Use of FSI for current wing simulations is expected to adequately predict the range of deformation on the MAV wing. As such, this paper analyzes the wing structure deformation, morphing forces and aerodynamic loads/derivatives, clarifying the proper correlation between wing deformation distribution and morphing forces as well as the potential benefits of membrane.

2.0 METHODOLOGY

2.1 Boundary conditions for MAV Wing model

The MAV wings (half wing) used for the structural analysis are presented in Figure 1. The baseline wings (rigid and membrane wings) and the washout TM (twist-morphing) wings (TM 5N, TM 3N and TM 1N wings) considered in this work have similar design dimensions and platform shape and were developed based on previous research by N.I. Ismail et al [16]. Each wing, whose physical properties and configurations are given in Table 1, has 1 mm thickness membrane skin component stretched about a frame, except the rigid wing. The inclusion of membrane skin onto the wing skeleton would permit gross deformation in wing shape in response to the subjected morphing forces[17]. Polymethyl methacrylate (also known as Perspex[18]) and silicone rubber[19] are utilized for the wing skeleton and membrane skin of the wings, respectively. Isotropic, homogeneous, and linearly elastic characteristics are assumed for all materials considered. The material properties of Perspex and rubber are listed in Table 2. Instead of a hyper elasticity material model, a linear elastic model is used for rubber material for simplification. Additionally, the flexible wing structures whose shapes are easily altered, required less force than a homogeneous wing (compared to rigid wing) for washout morphing. Generating washout twist morphing for the TM wings were achieved by enforcing 1N, 3N, and 5N at an optimized morphing location. Such forces were used to vary the y-direction displacement normal to the wing. The optimized morphing location is given in Figure 1 and is positioned at the wingtip and directed at 45° from XZ plane. This research excluded fuselage, stabilizers, and propeller components from the computational simulation.

DOI: https://doi.org/10.11113/jm.v46.488

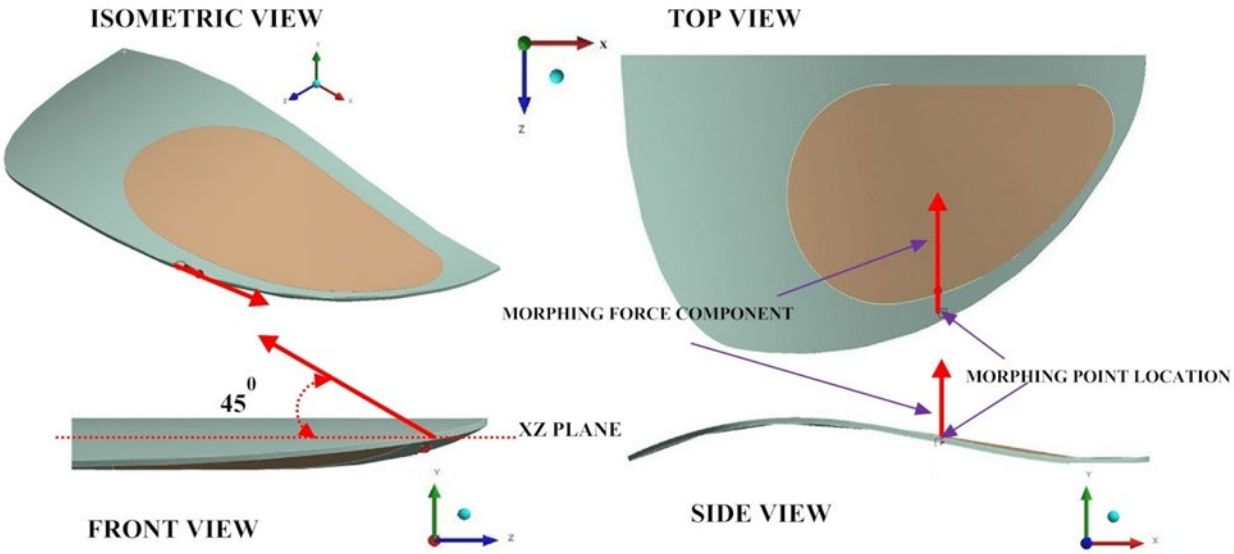

Figure 1: Morphing force imposed on TM Wing

Table 1: Design dimension and configuration for all wing types

Parameter	Rigid wing	Membrane wing	TM 1N	TM 3N	TM5N
Wingspan, b	150mm	150mm	150mm	150mm	150mm
Root chord, c	150mm	150mm	150mm	150mm	150mm
Aspect ratio, A	1.25	1.25	1.25	1.25	1.25
Maximum camber at the root	6.7% of c (at x/c =0.3)	6.7% of c (at x/c =0.3)	6.7% of c (at x/c =0.3)	6.7% of c (at x/c =0.3)	6.7% of c (at x/c =0.3)
Maximum reflex at the root	1.4% of c (at x/c = 0.86)	1.4% of c (at x/c = 0.86)	1.4% of c (at x/c = 0.86)	1.4% of c (at x/c = 0.86)	1.4% of c (at x/c = 0.86)
Built-in geometric twist	0.55°	0.55°	0.55°	0.55°	0.55°
Force component	Excluded	Excluded	F=1N	F=3N	F=5N
Membrane skin	Excluded	Included	Included	Included	Included

Table 1 Material properties of Perspex[18] and rubber[19]

Material name	Density (kg/m^3)	Young modulus (Pa)	Poisson's ratio	Bulk modulus (Pa)	Shear modulus (Pa)	Tensile Yield strength (Pa)
Perspex (polymethyl methacrylate)	1190	2.8×10^{9}	0.46	1.667×10^{10}	9.589×10^{8}	70
Rubber	1000	8.642×10^{6}	0.49	1.44×10^{8}	2.9×10^{6}	1.3787×10^{7}

2.2 Mesh Sensitivity Study

The selection of mesh, which serves as the foundation for numerical simulations, is a critical aspect of computational analysis in engineering and aerodynamics[20]. In this work, researchers conducted a mesh sensitivity study to assess the impact of various mesh element types on the accuracy and reliability of their results. Three distinct mesh types were considered in this study: coarse, intermediate, and fine meshes. An unstructured tetrahedral mesh type was chosen for their construction to ensure consistency and comparability across all wing models[21]. This mesh type

DOI: https://doi.org/10.11113/jm.v46.488

provides flexibility in accurately capturing the complex geometries of the wings. The primary goal of a mesh sensitivity study is to determine the grid independence of computational analysis. In a nutshell, it seeks to determine whether the results obtained from various mesh types converge and become consistent as the mesh size is refined. Grid independence is critical in numerical simulations because it ensures that the results are not overly influenced by mesh density[22], indicating that the chosen mesh adequately captures the underlying physical phenomena. In this study, the researchers chose a static structural analysis, to examine the structure responds to a load or force while at rest, with no dynamic motion. The results of this grid independence study are encapsulated in Figure 2, which serves as a visual representation of the findings. Notably, the optimized grid around 116,000 elements was chosen as the reference point for comparison. It is essential to highlight that the choice of this reference point was made based on the researchers' assessment of achieving a balanced trade-off between computational cost and accuracy.

Figure 2: Elements for static structural analysis of a (half) TM wing.

The results of the relative error and grid convergence index are compiled in Table 3, as crucial component of current case study. In the realm of computational simulations and numerical modelling, these metrics are importance to illuminate the precision and dependability of current computational approach[23]. In particular, the fine mesh configuration employed in this study has gained effectiveness and is acceptable. This evaluation is predicated primarily on the relative error, a fundamental measure of precision. In this instance, the relative error associated with the fine mesh is significantly below the 10 percent threshold[24], a widely accepted benchmark for acceptable simulation accuracy. The relative error is a quantitative measure of this simulation results match actual physical observations or experimental data. As this error falls below the 10% threshold, it indicates that the numerical model produces results that are sufficiently close to the actual behavior.

Table 3: Relative error and grid convergence index

Model Outputs	
Relative Error	1.93%
Extrapolated Relative Error	1.73%
Grid Convergence Index	1.87%

2.3 Validation Study

Based on experimental study conducted by N.I. Ismail et al. [17], Table 3 provides a comparison between experimentally measured wing tip deformations and those obtained through simulation for different morphing force levels (1N, 3N, and 5N). The relative error quantifies the difference between the experimental and simulated results as a percentage of the experimental value[25]. This data is to evaluate the accuracy of the simulation results in predicting the wing tip deformation under different morphing force levels. Wing tip deformation is used as a critical parameter, as it directly influences the aerodynamic performance and structural integrity of current works.

The table lists two sets of values for each of the three force levels (1N, 3N, and 5N): the measured wing tip deformation (in mm) obtained through experiments and the simulated wing tip deformation (also in mm) obtained through numerical simulations. The relative error is 0.3 percent

 DOI: https://doi.org/10.11113/jm.v46.488

for morphing forces of 1N. Accordingly, only 0.3 percent of the experimental measurement differs between the simulated and actual wing tip deformation. This result shows that the simulation and experiment for this force level were remarkably close to each other. The relative error decreases even more to 0.08 percent at 3N, a higher force level. It appears from this that the simulation, with only a small amount of variation from the experimental data, is remarkably accurate in predicting the wing tip deformation under this force. The relative error is 0.1 percent at a force level of 5N, too. The strong agreement between the simulation and experimental results is highlighted by the low relative error, which holds true even when the morphing forces are increased.

Table 3: Relative error for wing tip deformation values between N.I. Ismail et al. [17] and the present works

Morphing force	Wing tip deformation by N.I. Ismail et al. [17] (mm)	Wing tip deformation by simulation (mm)	Relative error
1N	3.15	3.14	0.3%
3N	11.7	11.71	0.08%
5N	19.5	19.52	0.1%

3.0 RESULTS AND DISCUSSION

3.1 Wing displacement results

The out of plane wing displacement results for all wings are presented in Figure 3. 3D wing displacement contours were visualized from the wing top view angle of the upper wing surfaces to capture the details magnitude of the displacement on y-axis. All wings were compared relatively between the AOA (angle of attack) cases with their respective location to demonstrate the wing deformation magnitude and deformation patterns. The wing displacement, normalized by the wing chord value (c= 0.15m) is calculated based on equation (1) which is taken from N.I. Ismail [17].

$$d_{max} = \left[\frac{(\text{maximum displacement magnitude at x/c = 0.4 to 1.0 area})}{\text{wing chord lenght}} \right] \times c \quad (1)$$

All the washout TM wings had considered the aerodynamic and morphing loads for the wing displacement since both of these factors contributed to the total wing deformations. The baseline wings (rigid and membrane wings), by contrast, were not subjected by morphing force and therefore deformed solely due to the aerodynamic force. Deformations are relatively insignificant for the rigid and membrane wing (d_{max} = 0.013c) with maximum displacement occurring at higher incidence angle (14° ~ 24°) at the leading edge. The measured membrane inflation ($1.0<2z/b<0.83$) which occurred due to aerodynamic force is very minimal and negligible, with no evident differences between the rigid and membrane wings.

As expected, the washout TM wings demonstrate a positive deflection (y-direction normal to the wing) of the wing tip, resulting a geometric twist of the wing. Nearly invariable maximum displacement magnitude (d_{max}) throughout each angle of attack cases can be observed with each wing experiencing maximum displacement at the wing tip (x/c = 0.6, 2z/b = 1.0).

Analyzing the deformations contour in Fig. 3, the TM 5N wing exhibits the highest displacement magnitude at d_{max} = 0.13c compared to other wings. This is followed by TM 3N and TM 1N wings which have slightly lower displacement at 0.078c and 0.021c, respectively. Such morphing force generally increases wing structural deformations, with the baseline wings differing than TM 1N wing on the order of 37%. This value can be expected to double when comparing the deformations magnitude of the TM 3N and TM 1N wings (74%). A comparison between TM 3N and TM 5N wings finds percentage changes of 40%. The structural deformation of the washout TM wings is

DOI: https://doi.org/10.11113/jm.v46.488

characterized by morphing load implemented at the wing tip: higher morphing force induced higher d_{max} magnitude.

Some displacement of the leading edge at low AOA (0° ~ 14°) can also be seen for the TM 5N and TM 3N wings, but not on TM 1N wing as leading-edge deformation occurred at higher AOA (20° ~ 24°). These are probably a result of the highly concentrated low-pressure cells at leading edge [17] with very high aerodynamic forces to cause a deflection.

4.0 CONCLUSION

The deformation patterns displayed by baseline wings and washout trailing-edge morphing (TM) wings are thoroughly examined in this research. Using sophisticated Ansys-FSI simulations, the paper explores their connections to morphing force and flying loads. The goal is to have a thorough grasp of how these wings react to different forces and how these reactions could affect the performance and design of MAV. The deformation patterns refer to the changes in the physical form and structure of the wings under various situations in the context of this study. These changes are important because it may influence the aircraft's aerodynamic performance, structural reliability, and overall performance. The study uses interconnected wing designs, including baseline wings, rigid wings, membrane wings, and washout TM wings, to analyze these patterns. The research's conclusions imply that the deformations in rigid and membrane wings are negligible, and the membrane frame shows no significant difference. On the other hand, the washout TM wings react very differently. When morphing force is applied at the wing tip, these washout TM wings exhibit substantial structural displacement. This obvious variation in behavior is important because it emphasizes how the morphing is affecting wing deformation. In-depth analysis of this phenomenon is provided in the study, along with information on the connection between morphing force and wing structural displacement. Notably, not all layouts exhibit the same amount of wing distortion. Instead, it fluctuates according to the magnitude morphing force. The TM 5N wing exhibits the maximum magnitude of displacement, making this variability particularly clear. This variation highlights the sensitivity of wing deformation towards the strength of external forces. Detailed analysis of the stated wing displacement trends leads to a solid conclusion. The effect of morphing force is proportional to the degree of wing deformation. The magnitude of structural wing displacement increases in proportion to the applied force. This knowledge is crucial for MAV designers and engineers, as it shows how varying loads and pressures affect the flight characteristics of aircraft wings.

DOI: https://doi.org/10.11113/jm.v46.488

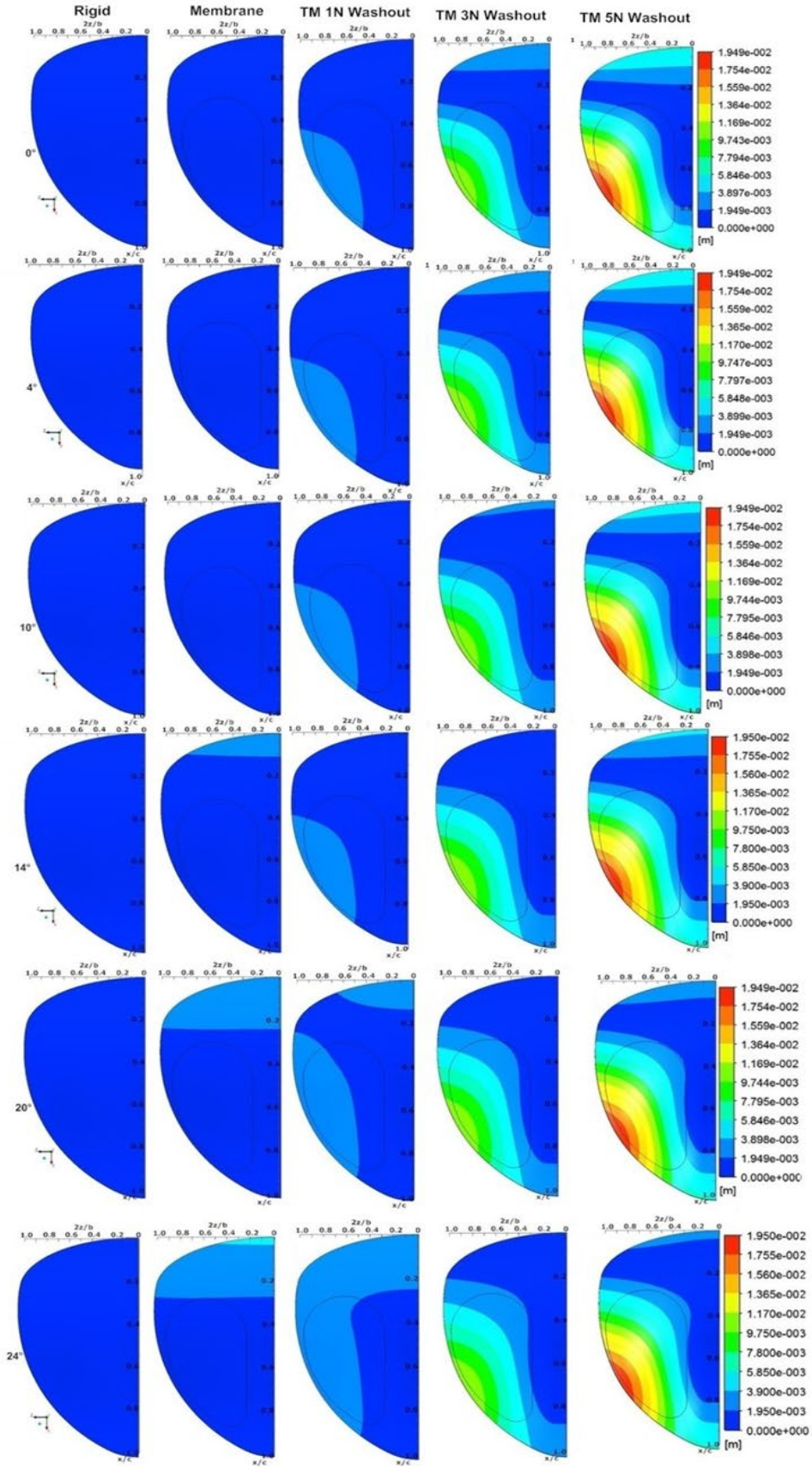

Figure 3: The 3D displacement contours for all wings at different angle of attack.

DOI: https://doi.org/10.11113/jm.v46.488

ACKNOWLEDGMENTS

Authors acknowledge technical and financial support from Universiti Teknologi MARA, Cawangan Pulau Pinang and the Government of Malaysia.

REFERENCES

1. Bachmann, Richard J., Ravi Vaidyanathan, Frank J. Boria, James Pluta, Josh Kiihne, Brian K. Taylor, Robert H. Bledsoe, Peter G. Ifju, and Roger D. Quinn, *A miniature vehicle with extended aerial and terrestrial mobility*: *Flying Insects and Robots.* 2009: Springer
2. Pornsin-sirirak, T. Nick, Yu-chong Tai, Chih-ming Ho, and Matt Keennon. *Microbat : A palm-sized electrically powered ornithopter in Proceedings of NASA/JPL Workshop on Biomorphic Robotics*. 2001.
3. Khambatta, Parvez, Lawrence Ukeiley, Charles Tinney, Bret Stanford, and Peter Ifju, *Flow characteristics of a three-dimensional fixed micro air vehicle wing.* American Institute of Aeronautics and Astronautics, 2008. **1**(6): p. 1–16.
4. Hassanalian, M., A. Quintana, and A. Abdelkefi, *Morphing and growing micro unmanned air vehicle : sizing process and stability.* Aerospace Science and Technology, 2018. **78**: p. 130–46.
5. Abudarag, Sakhr, Rashid Yagoub, Hassan Elfatih, and Zoran Filipovic, *Computational analysis of Unmanned Aerial Vehicle (UAV) in 2016 IEEE International Conference on Robotics and Automation (ICRA)*. 2017.
6. Phan, Hoang Vu, and Hoon Cheol Park, *Insect*-inspired, tailless, hover-capable flapping-wing robots: recent progress*, challenges, and future directions*. Progress in Aerospace Sciences, 2019. **111**(8): p. 100573.
7. Hamad, Ali Jihad, *Size and shape effect of specimen on the compressive strength of HPLWFC reinforced with glass fibres.* Journal of King Saud University - Engineering Sciences, 2017. **29**(4): p. 373–80.
8. Liang, Bin, and Mao Sun, *Aerodynamic interactions between wing and body of a model insect in forward flight and maneuvers.* Journal of Bionic Engineering, 2013. **10**(1): p. 19–27.
9. Ajanic, Enrico, Mir Feroskhan, Stefano Mintchev, Flavio Noca, and Dario Floreano, *Bioinspired wing and tail morphing extends drone flight capabilities*. Science Robotics, 2020. **5**(47).
10. Motazed, Ben, David Vos, and Mark Drela. *Aerodynamics and flight control design for hovering micro air vehicles in Proceedings Of The American Control Conference*. 1998.
11. Shang, J. K., S. A. Combes, B. M. Finio, and R. J. Wood, *Artificial insect wings of diverse morphology for flapping-wing micro air vehicles.* Bioinspiration & Biomimetics, 2009. **4**(3): p. 6.
12. Torres, Gabriel, and Thomas J. Mueller. *Micro aerial vehicle development: design, components, fabrication, and flight testing in AUVSI unmanned systems symposium and exhibition*. 2000.
13. Chen, Chen, and Tianyu Z,ang, *A review of design and fabrication of the bionic flapping wing micro air vehicles.* Micromachines, 2019. **10**(2).
14. Phan, Hoang Vu, Steven Aurecianus, Taesam Kang, and Hoon Cheol Park, *KUBeetle-S: An insect-like, tailless, hover-capable robot that can fly with a low-torque control mechanism*. International Journal of Micro Air Vehicles, 2019. **11**:1–10.
15. Abdulrahim, Mujahid, Helen Garcia, and Rick Lind, *Flight characteristics of shaping the membrane wing of a micro air vehicle*. journal of aircraft, 2005. **42**(1): p. 131–137.
16. Ismail, N. I., A. H. Zulkifli, M. Z. Abdullah, M. Hisyam Basri, and Norazharuddin Shah Abdullah, *Optimization of aerodynamic efficiency for twist morphing mav wing*, Chinese Journal of Aeronautics, 2014. **27**(3): p. 475–87.
17. Ismail, N. I., H. Yusoff, Hazim Sharudin, Arif Pahmi, H. Hafiz, and M. M. Mahadzir, *Lift distribution of washout twist morphing mav wing.* International Journal of Engineering and Technology(UAE), 2018. **7**(4): p. 89–94.
18. Typical physical properties, 2013. *Perspex Cast, Typical Physical Properties Flammability*, Available from:https://www.perspex.co.uk/Perspex/media/General/technical-library/Typical%20Physical%20Properties/Perspex-Acrylic-Typical-Physical-Properties.pdf [Accessed 02 August 2023]
19. Abudaram, Yaakov, Peter Ifju, James Hubner, and Lawrence Ukeiley, *Controlling pre-tension of silicone membranes on micro air vehicle flexible wings.* Journal of Strain Analysis for Engineering Design, 2012. **49**(1): p. 1–11.
20. Almohammadi, K. M., D. B. Ingham, L. Ma, and M. Pourkashan, *Computational Fluid Dynamics (CFD) mesh independency techniques for a straight blade vertical axis wind turbine.* Energy, 2013. **58**:483–93.
21. Baker, Nazar, Ger Kelly, and Paul D. O'Sulli,an, *A grid convergence index study of mesh style effect on the accuracy of the numerical results for an indoor airflow profile.* International Journal of Ventilation, 2020. **19**(4): p. 300–314.
22. Goetten, Falk, D. Felix, Matthew Marino, Cees Bil, Marc Havermann, and Carsten Braun. *A review of guidelines and best practices for subsonic aerodynamic simulations using RANS CFD in 11th Asia-Pacific International Symposium of Aerospace Technology,* 2019.
23. Seeni, Aravind, Parvathy Rajendran, and Hussin Mamat, *A CFD mesh independent solution technique for low reynolds number propeller.* CFD Letters, 2019. **11**(10):15–30.
24. Blokhuis, Alex, Philippe Nghe, Luca Peliti, and David Lacoste, *The generality of transient compartmentalization and its associated error thresholds.* Journal of Theoretical Biology, 2020. **487**: p. 110-110.

 DOI: https://doi.org/10.11113/jm.v46.488

25. Xie, Jingfeng, Jun Huang, Lei Song, Jingcheng Fu, and Xiaoqiang Lu, *An effort saving method to establish global aerodynamic model using CFD.* Aircraft Engineering and Aerospace Technology, 2022. **94**(11): p.1–19.

 DOI: https://doi.org/10.11113/jm.v46.488